Seismic reflection data interpolation with differential offset and shot continuation[a]

[a]Published in Geophysics, 68, 733-744 (2003)

Sergey Fomel

ABSTRACT

I propose a finite-difference offset continuation filter for interpolating seismic reflection data. The filter is constructed from the offset continuation differential equation and is applied on frequency slices in the log-stretch frequency domain. Synthetic and real data tests demonstrate that the proposed method succeeds in structurally complex situations where more simplistic approaches fail.

INTRODUCTION

Data interpolation is one of the most important problems of seismic data processing. In 2-D exploration, the interpolation problem arises because of missing near and far offsets, spatial aliasing and occasional bad traces. In 3-D exploration, the importance of this problem increases dramatically because 3-D acquisition almost never provides a complete regular coverage in both midpoint and offset coordinates (Biondi, 1999). Data regularization in 3-D can solve the problem of Kirchoff migration artifacts (Gardner and Canning, 1994), prepare the data for wave-equation common-azimuth imaging (Biondi and Palacharla, 1996), or provide the spatial coverage required for 3-D multiple elimination (van Dedem and Verschuur, 1998).

Claerbout (1992, 1999) formulates the following general principle of missing data interpolation:

> A method for restoring missing data is to ensure that the restored data, after specified filtering, has minimum energy.

How can one specify an appropriate filtering for a given interpolation problem? Smooth surfaces are conveniently interpolated with Laplacian filters (Briggs, 1974). Steering filters help us interpolate data with predefined dip fields (Clapp et al., 1998). Prediction-error filters in time-space or frequency-space domain successfully interpolate data composed of distinctive plane waves (Spitz, 1991; Claerbout, 1999). Local plane waves are handled with plane-wave destruction filters (Fomel, 2002). Because prestack seismic data is not stationary in the offset direction, non-stationary prediction-error filters need to be estimated, which leads to an accurate but relatively expensive method with many adjustable parameters (Crawley et al., 1999).

A simple model for reflection seismic data is a set of hyperbolic events on a common midpoint gather. The simplest filter for this model is the first derivative in the offset direction applied after the normal moveout correction. Going one step beyond this simple approximation requires taking the dip moveout (DMO) effect into account (Deregowski, 1986). The DMO effect is fully incorporated in the offset continuation differential equation (Fomel, 1994, 2003).

Offset continuation is a process of seismic data transformation between different offsets (Deregowski and Rocca, 1981; Bolondi et al., 1982; Salvador and Savelli, 1982). Different types of DMO operators (Hale, 1991) can be regarded as continuation to zero offset and derived as solutions of an initial-value problem with the revised offset continuation equation (Fomel, 2003). Within a constant-velocity assumption, this equation not only provides correct traveltimes on the continued sections, but also correctly transforms the corresponding wave amplitudes (Fomel et al., 1996). Integral offset continuation operators have been derived independently by Chemingui and Biondi (1994), Bagaini and Spagnolini (1996), and Stovas and Fomel (1996). The 3-D analog is known as azimuth moveout (AMO) (Biondi et al., 1998). In the shot-record domain, integral offset continuation transforms to shot continuation (Schwab, 1993; Bagaini and Spagnolini, 1993; Spagnolini and Opreni, 1996). Integral continuation operators can be applied directly for missing data interpolation and regularization (Bagaini et al., 1994; Mazzucchelli and Rocca, 1999). However, they don't behave well for continuation at small distances in the offset space because of limited integration apertures and, therefore, are not well suited for interpolating neighboring records. Additionally, as all integral (Kirchoff-type) operators they suffer from irregularities in the input geometry. The latter problem is addressed by accurate but expensive inversion to common offset (Chemingui, 1999).

In this paper, I propose an application of offset continuation in the form of a finite-difference filter for Claerbout's method of missing data interpolation. The filter is designed in the log-stretch frequency domain, where each frequency slice can be interpolated independently. Small filter size and easy parallelization among different frequencies assure a high efficiency of the proposed approach. Although the offset continuation filter lacks the predictive power of non-stationary prediction-error filters, it is much simpler to handle and serves as a good *a priori* guess of an interpolative filter for seismic reflection data. I first test the proposed method by interpolating randomly missing traces in a constant-velocity synthetic dataset. Next, I apply offset continuation and related shot continuation field to a real data example from the North Sea. Using a pair of offset continuation filters, operating in two orthogonal directions, I successfully regularize a 3-D marine dataset. These tests demonstrate that the offset continuation can perform well in complex structural situations where more simplistic approaches fail.

OFFSET CONTINUATION

A particularly efficient implementation of offset continuation results from a log-stretch transform of the time coordinate (Bolondi et al., 1982), followed by a Fourier transform of the stretched time axis. After these transforms, the offset continuation equation from (Fomel, 2003) takes the form

$$h\left(\frac{\partial^2 \tilde{P}}{\partial y^2}-\frac{\partial^2 \tilde{P}}{\partial h^2}\right)-i\,\Omega\,\frac{\partial \tilde{P}}{\partial h}=0\;, \tag{1}$$

where Ω is the corresponding frequency, h is the half-offset, y is the midpoint, and $\tilde{P}(y,h,\Omega)$ is the transformed data. As in other F-X methods, equation (1) can be applied independently and in parallel on different frequency slices.

We can construct an effective offset-continuation finite-difference filter by studying first the problem of wave extrapolation between neighboring offsets. In the frequency-wavenumber domain, the extrapolation operator is defined by solving the initial-value problem on equation (1). The solution takes the following form (Fomel, 2003):

$$\hat{\tilde{P}}(h_2)=\hat{\tilde{P}}(h_1)\,Z_\lambda(kh_2)/Z_\lambda(kh_1)\;, \tag{2}$$

where $\lambda=(1+i\Omega)/2$, and Z_λ is the special function defined as

$$\begin{aligned} Z_\lambda(x) &= \Gamma(1-\lambda)\left(\frac{x}{2}\right)^\lambda J_{-\lambda}(x)={}_0F_1\left(;1-\lambda;-\frac{x^2}{4}\right) \\ &= \sum_{n=0}^{\infty}\frac{(-1)^n}{n!}\,\frac{\Gamma(1-\lambda)}{\Gamma(n+1-\lambda)}\left(\frac{x}{2}\right)^{2n}\;, \end{aligned} \tag{3}$$

where Γ is the gamma function, $J_{-\lambda}$ is the Bessel function, and ${}_0F_1$ is the confluent hypergeometric limit function (Petkovsek et al., 1996). The wavenumber k in equation (2) corresponds to the midpoint y in the original data domain. In the high-frequency asymptotics, operator (2) takes the form

$$\hat{\tilde{P}}(h_2)=\hat{\tilde{P}}(h_1)\,F(2kh_2/\Omega)/F(2kh_1/\Omega)\,\exp\left[i\Omega\,\psi\left(2kh_2/\Omega-2kh_1/\Omega\right)\right]\;, \tag{4}$$

where

$$F(\epsilon)=\sqrt{\frac{1+\sqrt{1+\epsilon^2}}{2\sqrt{1+\epsilon^2}}}\,\exp\left(\frac{1-\sqrt{1+\epsilon^2}}{2}\right)\;, \tag{5}$$

and

$$\psi(\epsilon)=\frac{1}{2}\left(1-\sqrt{1+\epsilon^2}+\ln\left(\frac{1+\sqrt{1+\epsilon^2}}{2}\right)\right)\;. \tag{6}$$

Returning to the original domain, we can approximate the continuation operator with a finite-difference filter with the Z-transform

$$\hat{P}_{h+1}(Z_y)=\hat{P}_h(Z_y)\frac{G_1(Z_y)}{G_2(Z_y)}\;. \tag{7}$$

The coefficients of the filters $G_1(Z_y)$ and $G_2(Z_y)$ are found by fitting the Taylor series coefficients of the filter response around the zero wavenumber. In the simplest case of 3-point filters[1], this procedure uses four Taylor series coefficients and leads to the following expressions:

$$G_1(Z_y) = 1 - \frac{1 - c_1(\Omega)h_2^2 + c_2(\Omega)h_1^2}{6} + \frac{1 - c_1(\Omega)h_2^2 + c_2(\Omega)h_1^2}{12}\left(Z_y + Z_y^{-1}\right) , \quad (8)$$

$$G_2(Z_y) = 1 - \frac{1 - c_1(\Omega)h_1^2 + c_2(\Omega)h_2^2}{6} + \frac{1 - c_1(\Omega)h_1^2 + c_2(\Omega)h_2^2}{12}\left(Z_y + Z_y^{-1}\right) , \quad (9)$$

where

$$c_1(\Omega) = \frac{3\,(\Omega^2 + 9 - 4i\,\Omega)}{\Omega^2\,(3 + i\,\Omega)}$$

and

$$c_2(\Omega) = \frac{3\,(\Omega^2 - 27 - 8i\,\Omega)}{\Omega^2\,(3 + i\,\Omega)} .$$

Figure 1 compares the phase characteristic of the finite-difference extrapolators (7) with the phase characteristics of the exact operator (2) and the asymptotic operator (4). The match between different phases is poor for very low frequencies (left plot in Figure 1) but sufficiently accurate for frequencies in the typical bandwidth of seismic data (right plot in Figure 1).

Figure 2 compares impulse responses of the inverse DMO operator constructed by the asymptotic $\Omega - k$ operator with those constructed by finite-difference offset continuation. Neglecting subtle phase inaccuracies at large dips, the two images look similar, which provides an experimental evidence of the accuracy of the proposed finite-difference scheme.

When applied on the offset-midpoint plane of an individual frequency slice, the one-dimensional implicit filter (7) transforms to a two-dimensional explicit filter with the 2-D Z-transform

$$G(Z_y, Z_h) = G_1(Z_y) - Z_h G_2(Z_y) . \quad (10)$$

Convolution with filter (10) is the regularization operator that I propose to use for interpolating prestack seismic data.

APPLICATION

I start numerical testing of the proposed regularization first on a constant-velocity synthetic, where all the assumptions behind the offset continuation equation are valid.

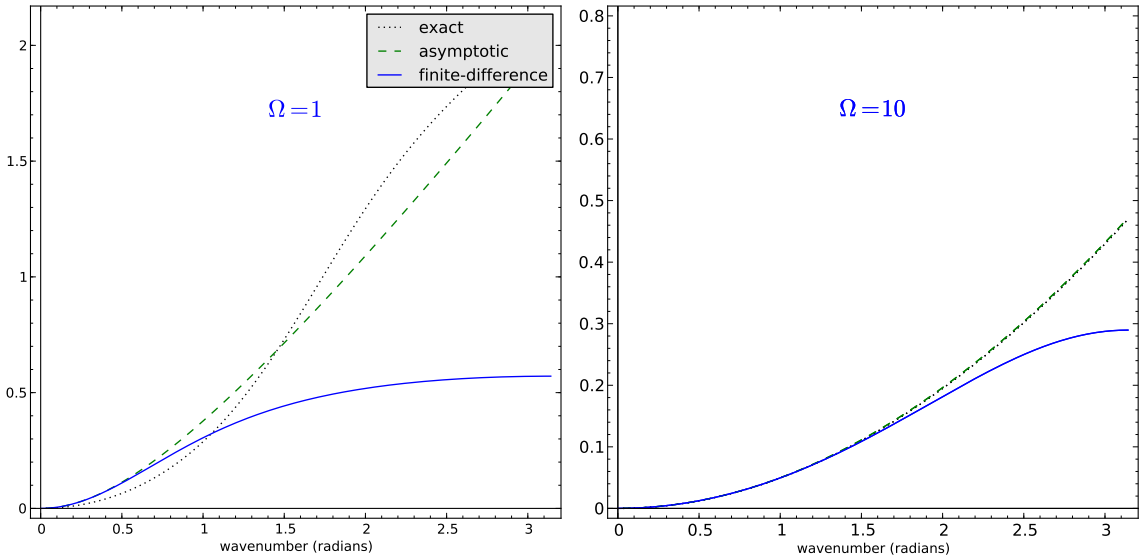

Figure 1: Phase of the implicit offset-continuation operators in comparison with the exact solution. The offset increment is assumed to be equal to the midpoint spacing. The left plot corresponds to $\Omega = 1$, the right plot to $\Omega = 10$.

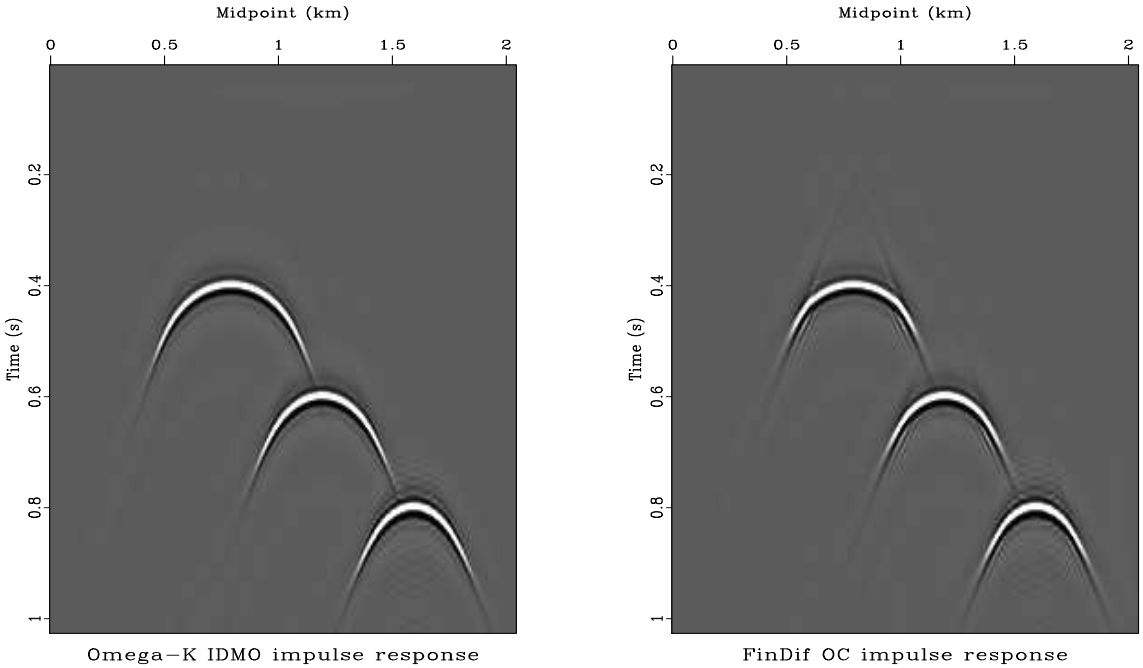

Figure 2: Inverse DMO impulse responses computed by the Fourier method (left) and by finite-difference offset continuation (right). The offset is 1 km.

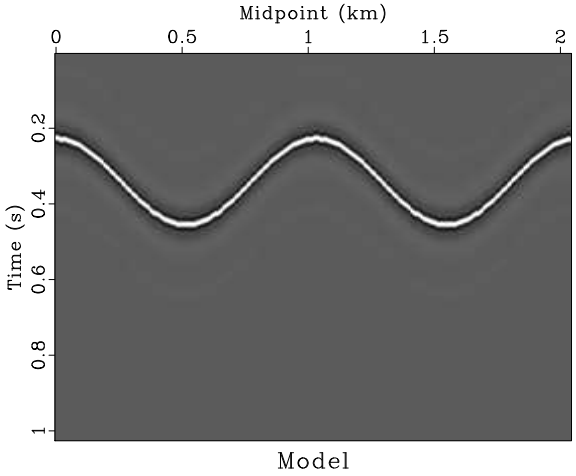

Figure 3: Reflector model for the constant-velocity test

Constant-velocity synthetic

A sinusoidal reflector shown in Figure 3 creates complicated reflection data, shown in Figures 4 and 5. To set up a test for regularization by offset continuation, I removed 90% of randomly selected shot gathers from the input data. The syncline parts of the reflector lead to traveltime triplications at large offsets. A mixture of different dips from the triplications would make it extremely difficult to interpolate the data in individual common-offset gathers, such as those shown in Figure 4. The plots of time slices after NMO (Figure 5) clearly show that the data are also non-stationary in the offset direction. Therefore, a simple offset interpolation scheme is also doomed.

Figure 6 shows the reconstruction process on individual frequency slices. Despite the complex and non-stationary character of the reflection events in the frequency domain, the offset continuation equation is able to accurately reconstruct them from the decimated data.

Figure 7 shows the result of interpolation after the data are transformed back to the time domain. The offset continuation result (right plots in Figure 7) reconstructs the ideal data (left plots in Figure 4) very accurately even in the complex triplication zones, while the result of simple offset interpolation (left plots in Figure 7) fails as expected. The simple interpolation scheme applied the offset derivative $\frac{\partial}{\partial h}$ in place of the offset continuation equation and thus did not take into account the movement of the events across different midpoints.

The constant-velocity test results allow us to conclude that, when all the assumptions of the offset continuation theory are met, it provides a powerful method of data regularization.

Being encouraged by the synthetic results, I proceed to a three-dimensional real data test.

[1]An analogous technique applied to the case of wavefield depth extrapolation with the wave equation would lead to the famous 45-degree implicit finite-difference operator (Claerbout, 1985).

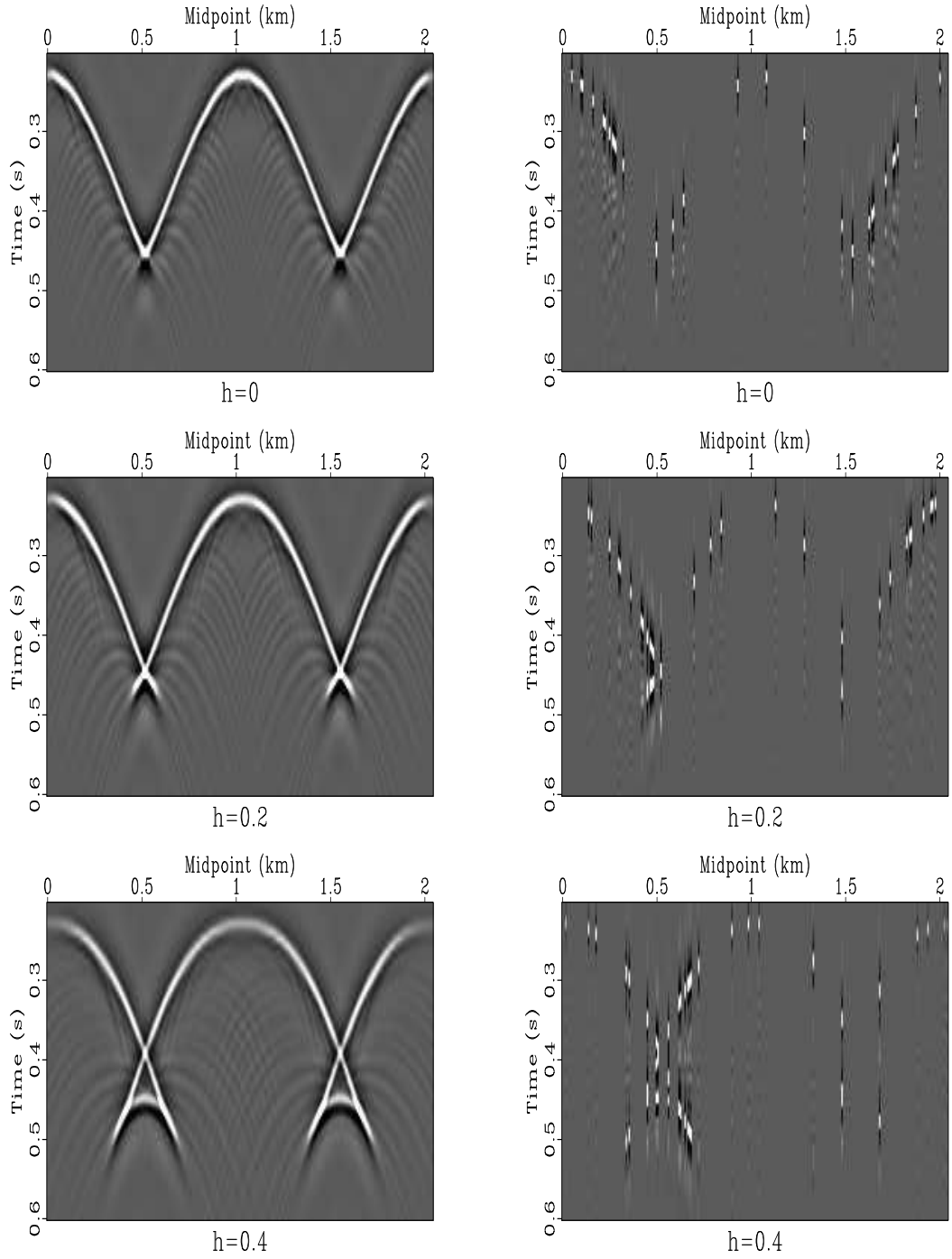

Figure 4: Prestack common-offset gathers for the constant-velocity test. Left: ideal data (after NMO). Right: input data (90% of shot gathers removed). Top, center, and bottom plots correspond to different offsets.

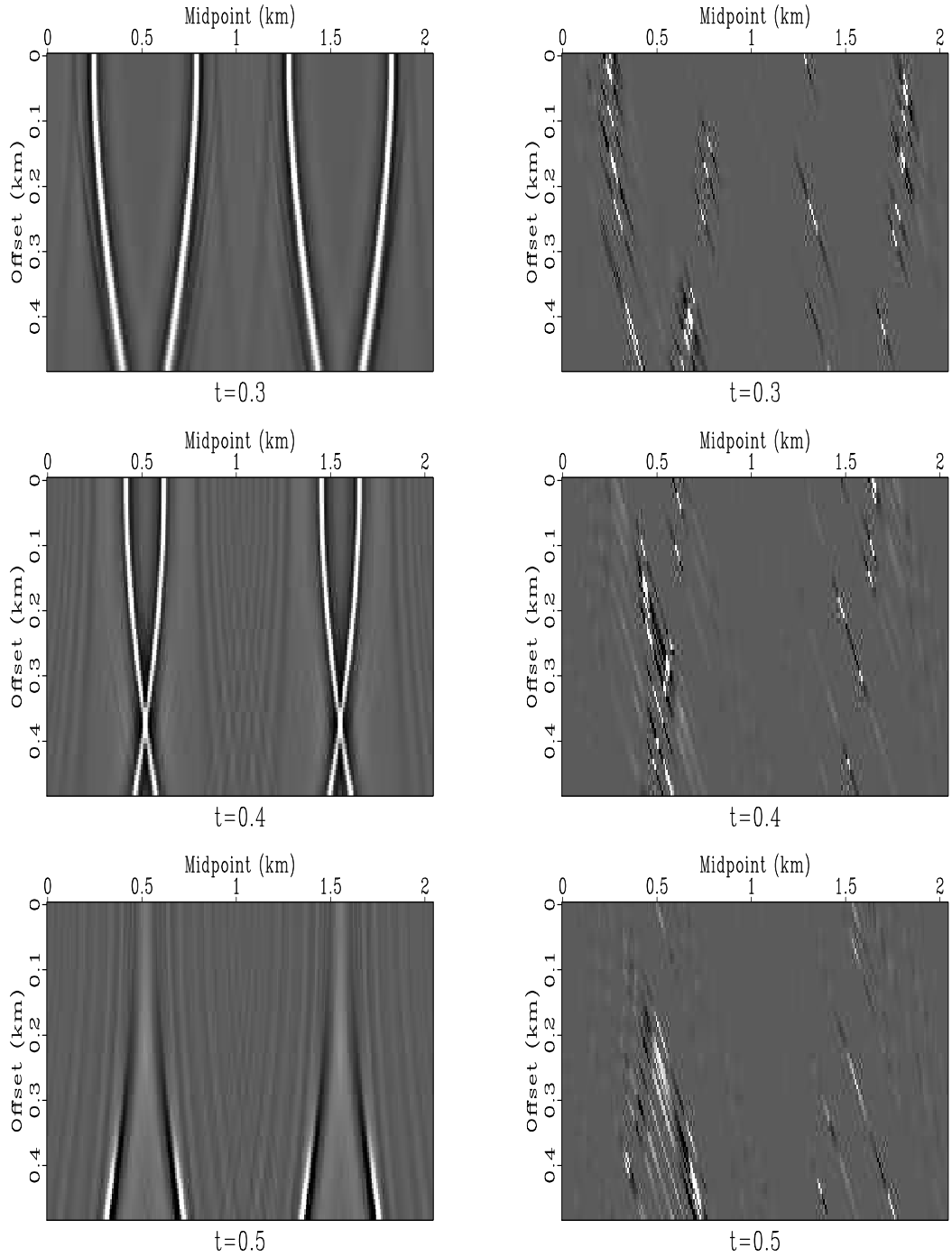

Figure 5: Time slices of the prestack data for the constant-velocity test. Left: ideal data (after NMO). Right: input data (90% of random gathers removed). Top, center, and bottom plots correspond to time slices at 0.3, 0.4, and 0.5 s.

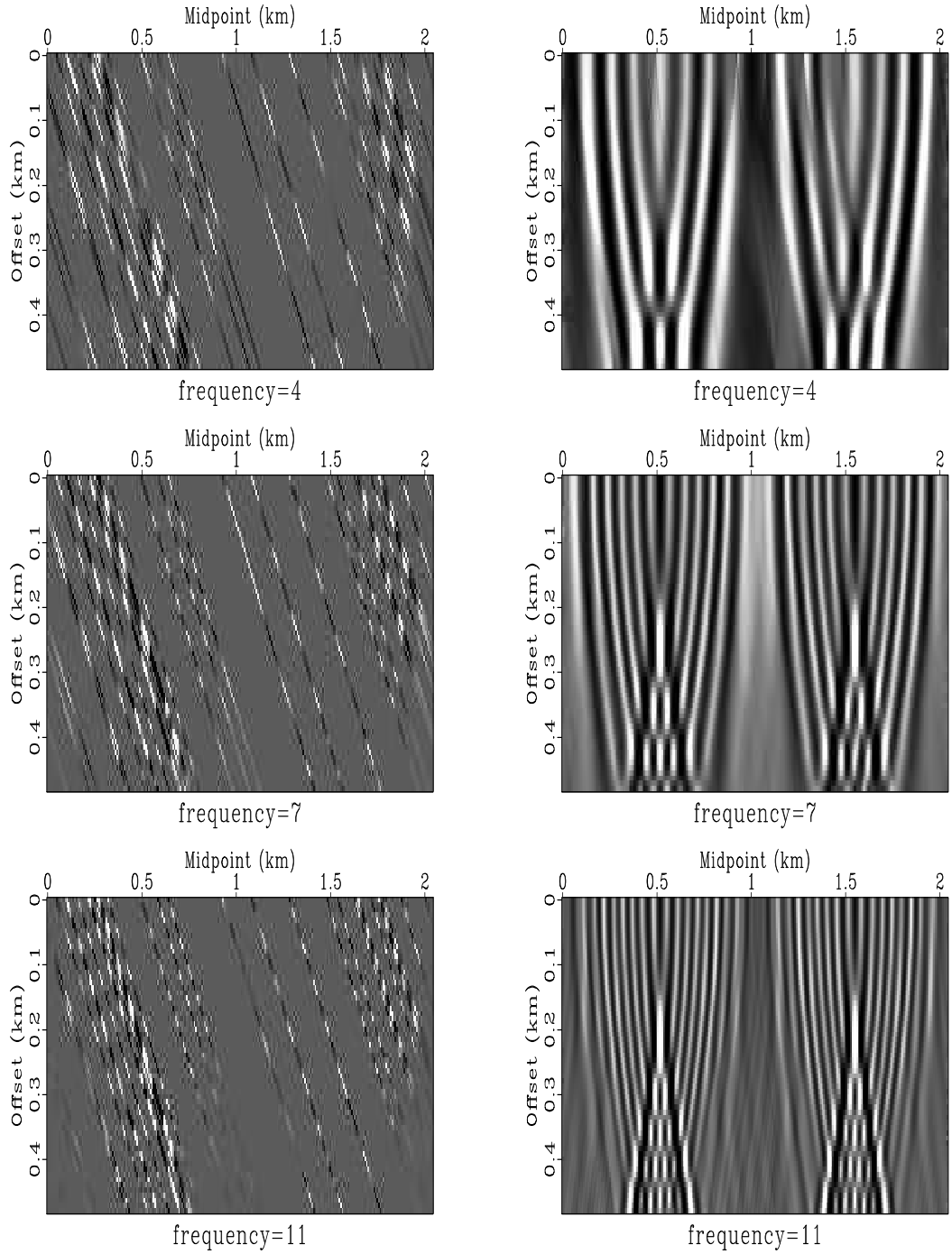

Figure 6: Interpolation in frequency slices. Left: input data (90% of the shot gathers removed). Right: interpolation output. Top, bottom, and middle plots correspond to different frequencies. The real parts of the complex-valued data are shown.

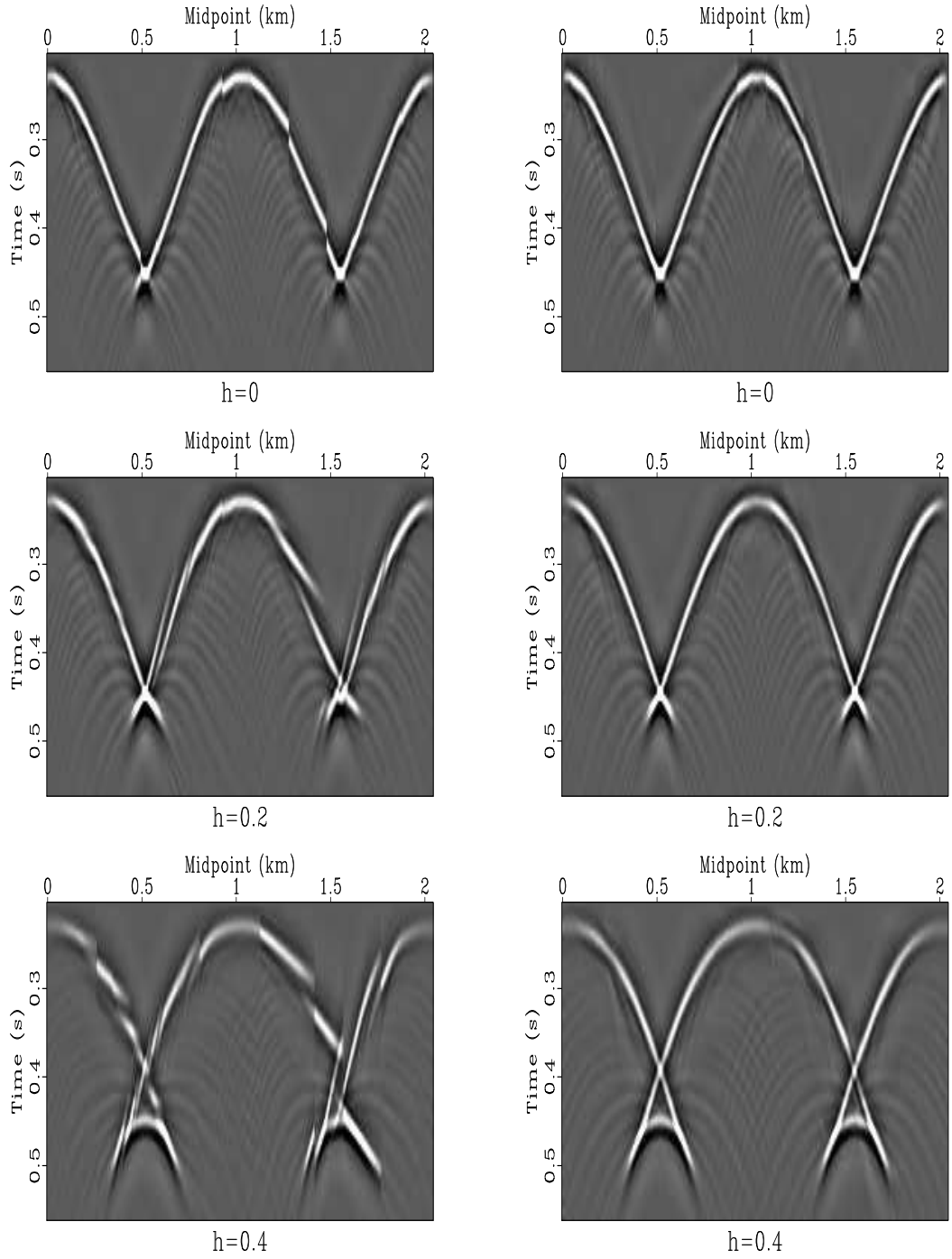

Figure 7: Interpolation in common-offset gathers. Left: output of simple offset interpolation. Right: output of offset continuation interpolation. Compare with Figure 4. Top, center, and bottom plots correspond to different common-offset gathers.

Analogously to integral azimuth moveout operator (Biondi et al., 1998), differential offset continuation can be applied in 3-D for regularizing seismic data prior to prestack imaging.

In the next section, I return to the 2-D case to consider an important problem of shot gather interpolation.

SHOT CONTINUATION

Missing or under-sampled shot records are a common example of data irregularity (Crawley, 2000). The offset continuation approach can be easily modified to work in the shot record domain. With the change of variables $s = y - h$, where s is the shot location, the frequency-domain equation (1) transforms to the equation

$$h \left(2 \frac{\partial^2 \tilde{P}}{\partial s \partial h} - \frac{\partial^2 \tilde{P}}{\partial h^2} \right) - i\,\Omega \left(\frac{\partial \tilde{P}}{\partial h} - \frac{\partial \tilde{P}}{\partial s} \right) = 0 \; . \tag{11}$$

Unlike equation (1), which is second-order in the propagation variable h, equation (11) contains only first-order derivatives in s. We can formally write its solution for the initial conditions at $s = s_1$ in the form of a phase-shift operator:

$$\hat{\tilde{P}}(s_2) = \hat{\tilde{P}}(s_1) \, \exp \left[i\, k_h \, (s_2 - s_1) \, \frac{k_h\, h - \Omega}{2\, k_h\, h - \Omega} \right] , \tag{12}$$

where the wavenumber k_h corresponds to the half-offset h. Equation (12) is in the mixed offset-wavenumber domain and, therefore, not directly applicable in practice. However, we can use it as an intermediate step in designing a finite-difference shot continuation filter. Analogously to the cases of plane-wave destruction and offset continuation, shot continuation leads us to the rational filter

$$\hat{P}_{s+1}(Z_h) = \hat{P}_s(Z_h) \frac{S(Z_h)}{\bar{S}(1/Z_h)} \; , \tag{13}$$

The filter is non-stationary, because the coefficients of $S(Z_h)$ depend on the half-offset h. We can find them by the Taylor expansion of the phase-shift equation (12) around zero wavenumber k_h. For the case of the half-offset sampling equal to the shot sampling, the simplest three-point filter is constructed with three terms of the Taylor expansion. It takes the form

$$S(Z_h) = -\left(\frac{1}{12} + i\, \frac{h}{2\,\Omega} \right) Z_h^{-1} + \left(\frac{2}{3} - i\, \frac{\Omega^2 + 12\, h^2}{12\, \Omega\, h} \right) + \left(\frac{5}{12} + i\, \frac{\Omega^2 + 18\, h^2}{12\, \Omega\, h} \right) Z_h \; . \tag{14}$$

Let us consider the problem of doubling the shot density. If we use two neighboring shot records to find the missing record between them, the problem reduces to the least-squares system

$$\left[\begin{array}{c} \mathbf{S} \\ \bar{\mathbf{S}} \end{array} \right] \mathbf{p}_s \approx \left[\begin{array}{c} \bar{\mathbf{S}}\, \mathbf{p}_{s-1} \\ \mathbf{S}\, \mathbf{p}_{s+1} \end{array} \right] \; , \tag{15}$$

where $\mathbf{S}$ denotes convolution with the numerator of equation (13), $\bar{\mathbf{S}}$ denotes convolution with the corresponding denominator, $\mathbf{p}_{s-1}$ and $\mathbf{p}_{s+1}$ represent the known shot gathers, and $\mathbf{p}_s$ represents the gather that we want to estimate. The least-squares solution of system (15) takes the form

$$\mathbf{p}_s = \left(\mathbf{S}^T\,\mathbf{S} + \bar{\mathbf{S}}^T\,\bar{\mathbf{S}}\right)^{-1}\,\left(\mathbf{S}^T\,\bar{\mathbf{S}}\,\mathbf{p}_{s-1} + \bar{\mathbf{S}}^T\,\mathbf{S}\,\mathbf{p}_{s+1}\right)\ . \tag{16}$$

If we choose the three-point filter (14) to construct the operators $\mathbf{S}$ and $\bar{\mathbf{S}}$, then the inverted matrix in equation (16) will have five non-zero diagonals. It can be efficiently inverted with a direct banded matrix solver using the LDL^T decomposition (Golub and Van Loan, 1996). Since the matrix does not depend on the shot location, we can perform the decomposition once for every frequency so that only a triangular matrix inversion will be needed for interpolating each new shot. This leads to an extremely efficient algorithm for interpolating intermediate shot records.

Sometimes, two neighboring shot gathers do not fully constrain the intermediate shot. In order to add an additional constraint, I include a regularization term in equation (16), as follows:

$$\mathbf{p}_s = \left(\mathbf{S}^T\,\mathbf{S} + \bar{\mathbf{S}}^T\,\bar{\mathbf{S}} + \epsilon^2\,\mathbf{A}^T\mathbf{A}\right)^{-1}\,\left(\mathbf{S}^T\,\bar{\mathbf{S}}\,\mathbf{p}_{s-1} + \bar{\mathbf{S}}^T\,\mathbf{S}\,\mathbf{p}_{s+1}\right)\ , \tag{17}$$

where $\mathbf{A}$ represents convolution with a three-point prediction-error filter (PEF), and ϵ is a scaling coefficient. The appropriate PEF can be estimated from $\mathbf{p}_{s-1}$ and $\mathbf{p}_{s+1}$ using Burg's algorithm (Burg, 1972, 1975; Claerbout, 1976). A three-point filter does not break the five-diagonal structure of the inverted matrix. The PEF regularization attempts to preserve offset dip spectrum in the under-constrained parts of the estimated shot gather.

Figure 9 shows the result of a shot interpolation experiment using the constant-velocity synthetic from Figure 4. In this experiment, I removed one of the shot gathers from the original NMO-corrected data and interpolated it back using equation (17). Subtracting the true shot gather from the reconstructed one shows a very insignificant error, which is further reduced by using the PEF regularization (right plots in Figure 9). The two neighboring shot gathers used in this experiment are shown in the top plots of Figure 8. For comparison, the bottom plots in Figure 8 show the simple average of the two shot gathers and its corresponding prediction error. As expected, the error is significantly larger than the error of shot continuation. An interpolation scheme based on local dips in the shot direction would probably achieve a better result, but it is significantly more expensive than the shot continuation scheme introduced above.

A similar experiment with real data from a North Sea marine dataset is reported in Figure 11. I removed and reconstructed a shot gather from the two neighboring gathers shown in Figure 10. The lower parts of the gathers are complicated by salt dome reflections and diffractions with conflicting dips. The simple average of the two input shot gathers (bottom plots in Figure 11) works reasonably well for nearly flat reflection events but fails to predict the position of the back-scattered diffractions

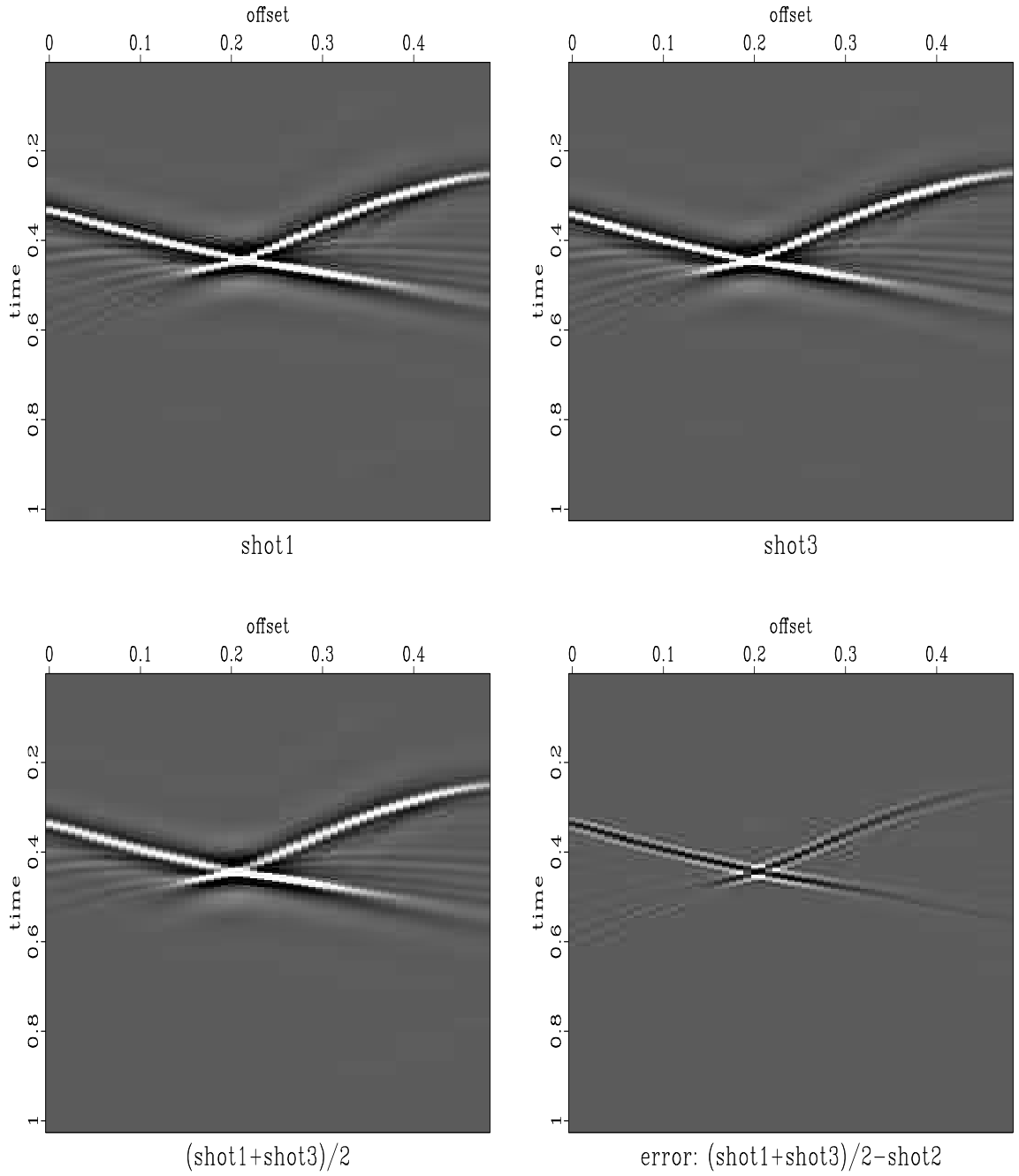

Figure 8: Top: Two synthetic shot gathers used for the shot interpolation experiment. An NMO correction has been applied. Bottom: simple average of the two shot gathers (left) and its prediction error (right).

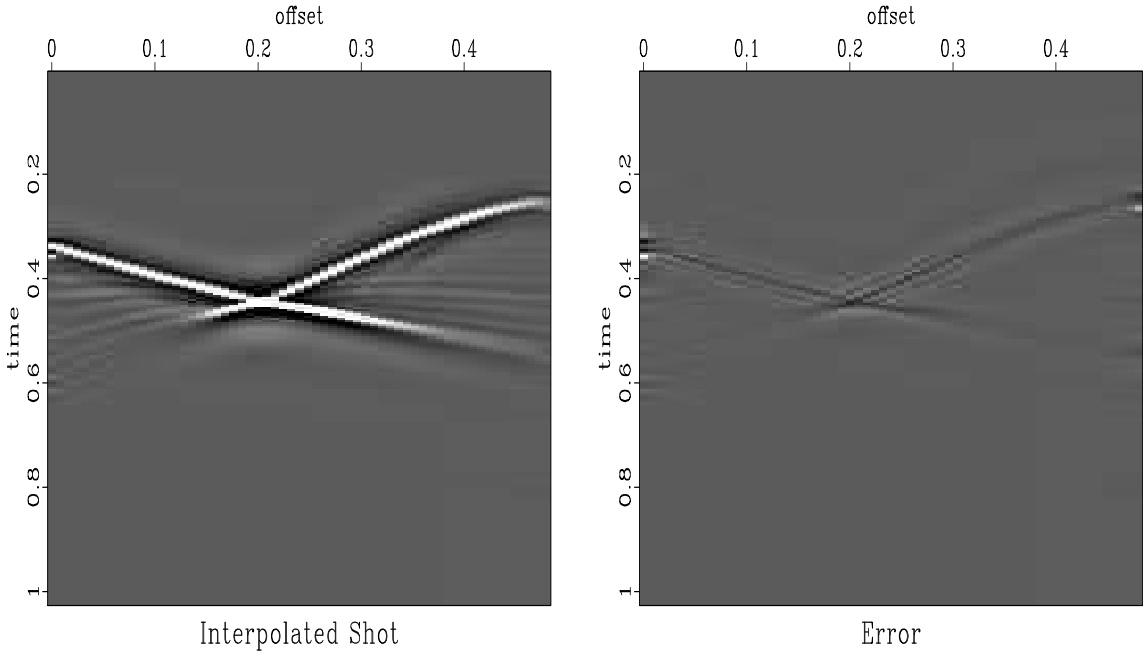

Figure 9: Synthetic shot interpolation results. Left: interpolated shot gathers. Right: prediction errors (the differences between interpolated and true shot gathers), plotted on the same scale.

events. The shot continuation method works well for both types of events (top plots in Figure 11). There is some small and random residual error, possibly caused by local amplitude variations.

Analogously to the case of offset continuation, it is possible to extend the shot continuation method to three dimensions. A simple modification of the proposed technique would also allow us to use more than two shot gathers in the input or to extrapolate missing shot gathers at the end of survey lines.

CONCLUSIONS

Differential offset continuation provides a valuable tool for interpolation and regularization of seismic data. Starting from analytical frequency-domain solutions of the offset continuation differential equation, I have designed accurate finite-difference filters for implementing offset continuation as a local convolutional operator. A similar technique works for shot continuation across different shot gathers. Missing data are efficiently interpolated by an iterative least-squares optimization. The differential filters have an optimally small size, which assures high efficiency.

Differential offset continuation serves as a bridge between integral and convolutional approaches to data interpolation. It shares the theoretical grounds with the integral approach but is applied in a manner similar to that of prediction-error filters

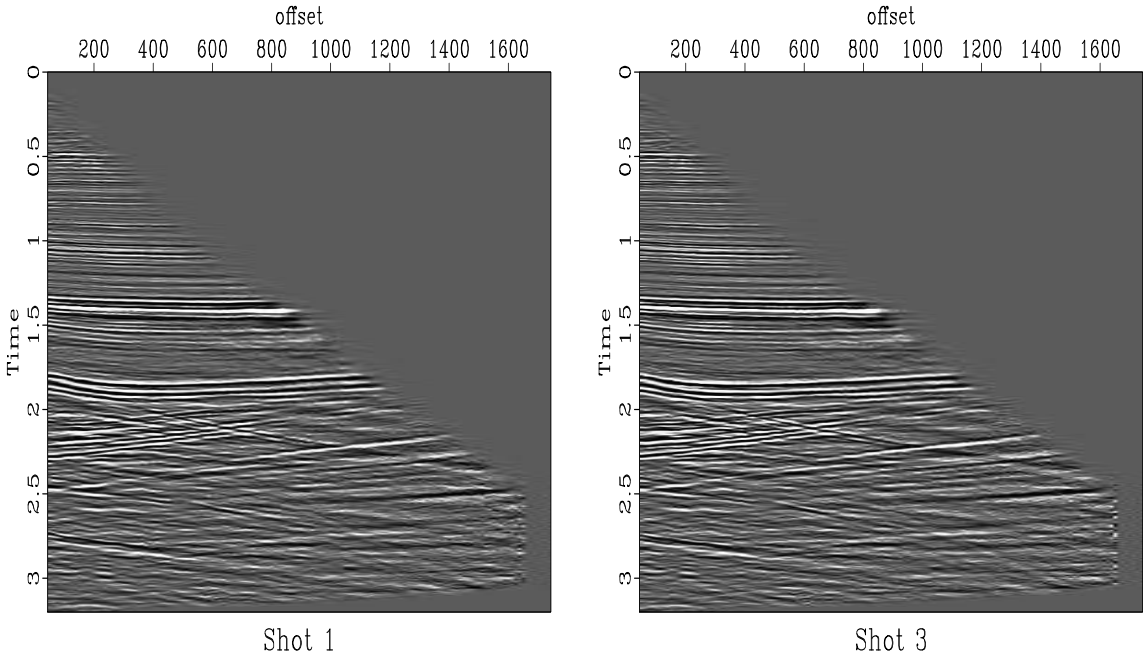

Figure 10: Two real marine shot gathers used for the shot interpolation experiment. An NMO correction has been applied.

in the convolutional approach.

Tests with synthetic and real data demonstrate that the proposed interpolation method can succeed in complex structural situations where more simplistic methods fail.

ACKNOWLEDGMENTS

The financial support for this work was provided by the sponsors of the Stanford Exploration Project (SEP).

For the shot continuation test, I used a North Sea dataset, released to SEP by Elf Aquitaine.

I thank Jon Claerbout and Biondo Biondi for helpful discussions about the practical application of differential offset continuation.

REFERENCES

Bagaini, C., and U. Spagnolini, 1993, Common shot velocity analysis by shot continuation operator: 63rd Ann. Internat. Mtg, Soc. of Expl. Geophys., 673–676.

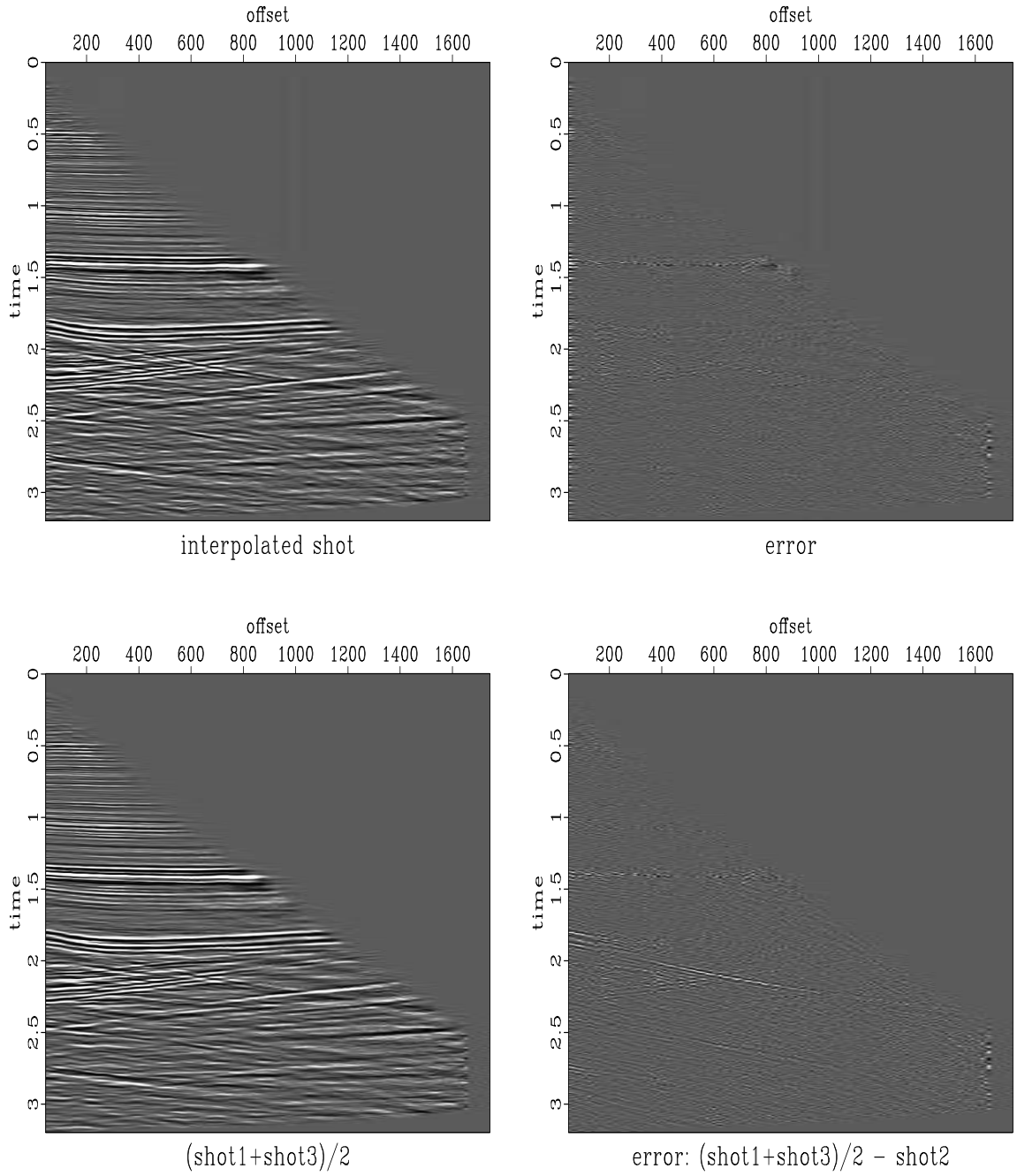

Figure 11: Real-data shot interpolation results. Top: interpolated shot gather (left) and its prediction error (right). Bottom: simple average of the two input shot gathers (left) and its prediction error (right).

———, 1996, 2-D continuation operators and their applications: Geophysics, **61**, 1846–1858.

Bagaini, C., U. Spagnolini, and V. P. Pazienza, 1994, Velocity analysis and missing offset restoration by prestack continuation operators: 64th Ann. Internat. Mtg, Soc. of Expl. Geophys., 1549–1552.

Biondi, B., S. Fomel, and N. Chemingui, 1998, Azimuth moveout for 3-D prestack imaging: Geophysics, **63**, 574–588.

Biondi, B., and G. Palacharla, 1996, 3-D prestack migration of common-azimuth data: Geophysics, **61**, 1822–1832.

Biondi, B. L., 1999, 3-D Seismic Imaging: Stanford Exploration Project.

Bolondi, G., E. Loinger, and F. Rocca, 1982, Offset continuation of seismic sections: Geophys. Prosp., **30**, 813–828.

Briggs, I. C., 1974, Machine contouring using minimum curvature: Geophysics, **39**, 39–48.

Burg, J. P., 1972, The relationship between maximum entropy spectra and maximum likelihood spectra (short note): Geophysics, **37**, 375–376.

———, 1975, Maximum entropy spectral analysis: PhD thesis, Stanford University.

Chemingui, N., 1999, Imaging irregularly sampled 3D prestacked data: PhD thesis, Stanford University.

Chemingui, N., and B. Biondi, 1994, Coherent partial stacking by offset continuation of 2-D prestack data, *in* SEP-82: Stanford Exploration Project, 117–126.

Claerbout, J., 1999, Geophysical estimation by example: Environmental soundings image enhancement: Stanford Exploration Project.

Claerbout, J. F., 1976, Fundamentals of geophysical data processing: Blackwell.

———, 1985, Imaging the Earth's Interior: Blackwell Scientific Publications.

———, 1992, Earth Soundings Analysis: Processing Versus Inversion: Blackwell Scientific Publications.

Clapp, R. G., B. L. Biondi, S. B. Fomel, and J. F. Claerbout, 1998, Regularizing velocity estimation using geologic dip information: 68th Ann. Internat. Mtg, Soc. of Expl. Geophys., 1851–1854.

Crawley, S., 2000, Seismic trace interpolation with nonstationary prediction-error filters: PhD thesis, Stanford University.

Crawley, S., J. Claerbout, and R. Clapp, 1999, Interpolation with smoothly nonstationary prediction-error filters: 69th Ann. Internat. Mtg, Soc. of Expl. Geophys., 1154–1157.

Deregowski, S. M., 1986, What is DmO: First Break, **04**, 7–24.

Deregowski, S. M., and F. Rocca, 1981, Geometrical optics and wave theory of constant offset sections in layered media: Geophys. Prosp., **29**, 374–406.

Fomel, S., 2002, Applications of plane-wave destruction filters: Geophysics, **67**, 1946–1960.

———, 2003, Theory of differential offset continuation: Geophysics, **68**, 718–732.

Fomel, S., N. Bleistein, H. Jaramillo, and J. K. Cohen, 1996, True amplitude DmO, offset continuation and AvA/AvO for curved reflectors: 66th Ann. Internat. Mtg, Soc. of Expl. Geophys., 1731–1734.

Fomel, S. B., 1994, Kinematically equivalent differential operator for offset continua-

tion of seismic sections: Russian Geology and Geophysics, **35**, 122–134.
Gardner, G. H. F., and A. Canning, 1994, Effects of irregular sampling on 3-D prestack migration: 64th Ann. Internat. Mtg, Soc. of Expl. Geophys., 1553–1556.
Golub, G. H., and C. F. Van Loan, 1996, Matrix computations: The John Hopkins University Press.
Hale, D., 1991, Dip Moveout Processing: Soc. of Expl. Geophys.
Mazzucchelli, P., and F. Rocca, 1999, Regularizing land acquisitions using shot continuation operators: effects on amplitudes: 69th Ann. Internat. Mtg, Soc. of Expl. Geophys., 1995–1998.
Petkovsek, M., H. S. Wilf, and D. Zeilberger, 1996, $A = B$: A K Peters Ltd.
Salvador, L., and S. Savelli, 1982, Offset continuation for seismic stacking: Geophys. Prosp., **30**, 829–849.
Schwab, M., 1993, Shot gather continuation, *in* SEP-77: Stanford Exploration Project, 117–130.
Spagnolini, U., and S. Opreni, 1996, 3-D shot continuation operator: 66th Ann. Internat. Mtg, Soc. of Expl. Geophys., 439–442.
Spitz, S., 1991, Seismic trace interpolation in the F-X domain: Geophysics, **56**, 785–794.
Stovas, A. M., and S. B. Fomel, 1996, Kinematically equivalent integral DMO operators: Russian Geology and Geophysics, **37**, 102–113.
van Dedem, E. J., and D. J. Verschuur, 1998, 3-D surface-related multiple elimination and interpolation: 68th Ann. Internat. Mtg, Soc. of Expl. Geophys., 1321–1324.